ACS OMEGA

Open Access

This article is licensed under CC-BY-NC-ND 4.0

http://pubs.acs.org/journal/acsodf

Article

Experimental Study on the Effect of Gas Pressure on the Pore Structure and Dynamic Mechanical Properties of Coal

Xin Gao, Sheng Xue,* Weiyu Li, Yidan Han, and Guangcheng Liu

Cite This: *ACS Omega* 2024, 9, 10468−10477

Read Online

ACCESS | Metrics & More | Article Recommendations

ABSTRACT: Understanding the effect of gas pressure on coal pore structure and dynamic mechanical properties can better guide the accurate monitoring of stress and gas in gas-containing coal seams in coal mines and efficiently prevent and control coal/rock-gas composite dynamic hazards. In this study, the characterization of the pore structure of the coal body under different gas pressures and three-dimensional impact compression tests were carried out. The findings demonstrate that when the axial static load and confining pressure are fixed, the gas pressure determines the amount of gas adsorbed by the coal samples and its pore structure changes. The effect of gas pressure on the pore structure of the micropores is not obvious, but it has an obvious dilatation effect on the pore structure of the macropores. Within the range of conditions and gas pressures studied in this paper, gas-containing coals' dynamic compressive strength and failure strain decrease linearly with increasing gas pressure. The average dynamic strength deterioration rate of gas-containing coals increases linearly with an increase of gas pressure, which plays a deteriorating role in the dynamic mechanical properties of coal bodies. When the gas pressure increases from 0.7 to 2.8 MPa, the radius of the macropores inside the gas-containing coal increases 0.63 times, and the increased pores and cracks produce a stress concentration effect around the pores and cracks and the shorter time required for instability damage of the coal samples to occur when subjected to dynamic loading. The research results improve the basic theory of gas-containing coal dynamics and provide a theoretical basis for the mine coal/rock-gas composite dynamics disaster.

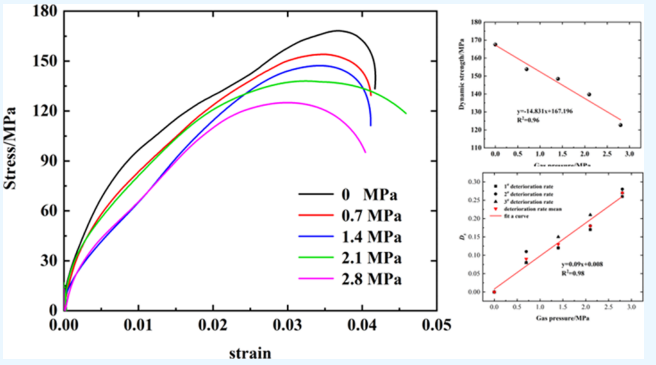

1. INTRODUCTION

Coal will remain the main source of energy in China for some time to come.[1] Compared with the world's major coal-producing countries, China's coal production method is dominated by shaft mining. Due to the complex conditions of shaft mining, China has long faced a more severe overall production safety posture for its coal resources.[2,3] In the process of coal mining, the coal body in front of the mining workings is disturbed by the stress caused by mining on the one hand, which leads to the redistribution of the internal stress of the coal body and the change of the state of the gas endowment.[4] On the other hand, the dynamic load generated by the periodic breakage of the roof plate in the mining area leads to the deformation and even the destruction of the gas-containing coal seams,[5,6] thus causing composite coal/rock kinetic hazards such as rock bursts or coal and gas outburst[7−9] Coal/rock-gas composite kinetic hazard accidents can cause direct injuries such as people being buried under pressure and smashed, or indirect injuries such as asphyxiation and gas explosions, posing a serious threat to coal mine safety. To prevent and reduce the occurrence of such accidents, it is especially important to deepen the understanding of the occurrence mechanism and process of coal/rock composite dynamic disaster, to master the change law of pore structure and the mechanism of destabilization damage of gas-containing coal under the mining environment, and to study the microscopic pore characteristics of gas-containing coal as well as to carry out the dynamic and static combined loading mechanical test of gas-containing coal.

To study the effect of gas pressure on the structural change characteristics of the internal pores of coal, many scholars have done much experimental research on this. In recent years, not much research has been done on the use of NMR technology in the field of coal, and some scholars have utilized low-field nuclear magnetic resonance (NMR) technology to study the structural change characteristics of coal bodies affected by different pressures.[10,11] To study the effect of gas on the microstructure of coal/rock bodies under a stress state, Liu et

Received: October 28, 2023
Revised: December 30, 2023
Accepted: January 8, 2024
Published: February 21, 2024

© 2024 The Authors. Published by American Chemical Society

al.[12] and others conducted gas adsorption tests on raw coal samples under different gas pressure conditions using nuclear magnetic resonance (NMR) technology. The results showed that with the increase of gas pressure, the coal samples reached adsorption equilibrium for a longer period of time and had a significant expansion of the medium and large pores. Yang et al.[13] conducted gas adsorption experiments on coal samples under different enclosing pressure conditions using a low-field nuclear magnetic resonance system and enclosing pressure system. The results showed that increasing confining pressure has an obvious contraction effect on medium and large pore structures, while the effect on micro- and small pore structures is not obvious. Xu and Wu[14] carried out gas adsorption tests on coal samples under different gas pressure conditions using a nuclear magnetic resonance (NMR) device, and the results showed that with the increase of gas pressure, new pores would be generated inside the coal body, and the pores would be connected with each other to form fissures, and the porosity of the coal samples would then increase. Numerous scholars have made preliminary explorations on the internal pore and fracture changes of gas-containing coals, and the research results show that the pore and fracture structures of underground coal/rock bodies are subjected to the combined effects of gas pressure and stress at the same time.

In addition, the underground stress and gas pressure will also have a certain effect on the mechanical properties of coal/rock.[15−17] Based on this, Gao et al.[18] used an acoustic emission analysis tester to study the mechanical properties of gas-containing coal samples under uniaxial compressive loading and the acoustic emission signal evolution law. Wang et al.[19] investigated the change characteristics of stress−strain curves, mechanical properties, and dynamic fracture evolution laws of gas-containing coal samples at different deformation stages under triaxial compression conditions using an industrial CT scanning system of affected coal/rock. Liang et al.[20] illustrated the mechanical and nonmechanical effects of gas on the mechanical properties and ontological relationships of coal by conducting triaxial compression tests on coal under different pore gas pressures, which showed that the modulus of elasticity and the strength of the coal body were reduced by adsorbing gas. Yin et al.[21] investigated the mechanical properties (i.e., uniaxial compressive strength, tensile strength, and fracture toughness) of gas-containing coals with initial gas pressures of 0, 0.5, 1, and 1.5 MPa, respectively. The results showed that the uniaxial compressive strength, tensile strength, and fracture toughness of gas-containing coal decreased with the increase in initial gas pressure. Currently, most of the studies on the mechanical properties of gas-containing coals are inclined to static mechanics, but in the mining of coal resources, artificial disturbances such as fracture of the roof slab overlying the mining area and rock blasting will produce apparent dynamic phenomena.[22−25] The coal body, in this case, will be subjected to dynamic loads along with tectonic stresses and pore pressure in the coal body. When coal/rock is subjected to the multifield coupling effect of underground stress, gas pressure, and quarry disturbance stress, it is easy to trigger the occurrence of disasters such as rock burst or coal and gas outburst.

Based on this, this paper utilizes the nuclear magnetic resonance (NMR) analysis tester and the self-developed dynamic and static combined loading dynamics test system of gas-containing coal to carry out gas adsorption experiments and impact dynamic tests on coal samples under triaxial loading and to investigate the effects of the pore characteristics and dynamic mechanical properties of gas-containing coals and the influence of the pore characteristics on the dynamic mechanical properties of coal samples under the coupling effect of the underground stress and the gas pressures. The study results are of great theoretical significance in revealing the pore structure characteristics and changing law of dynamic mechanical indexes of gas-containing coal.

2. TESTS AND METHODS

2.1. Specimen Preparation. The coal samples selected for the test were from the Han Jiawan coal mine in Yulin, Shanxi Province, China. To minimize the test error, we chose the same coal seam, the same area of the large pieces of raw coal for sampling, and the large amounts of coal samples into the test chamber and processed into two kinds of models of the size of Φ50 mm × 25 mm and Φ25 mm × 50 mm, with specimen ends of the nonparallelism of the surface of 0.02 mm or less. To minimize the dispersion of the coal samples, the wave velocity test was performed on the coal samples, and coal samples with similar density were selected for the test, during which butter was applied to the ends of the coal samples to reduce the friction effect. NMR and impact dynamics tests were performed on the selected coal samples of two sizes, respectively. The coal sample preparation and test procedure are shown in Figure 1.

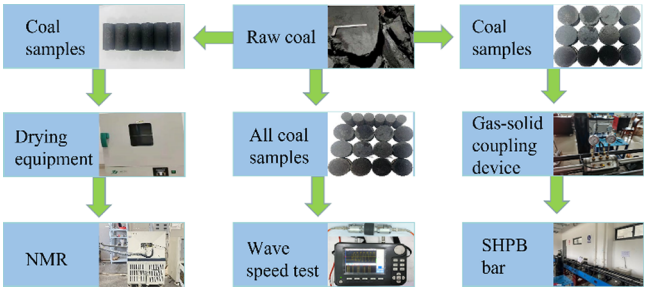

Figure 1. Specimen preparation and experimental procedure.

2.2. Experimental Study on the Changing Law of Pore Characteristics of Gas-Containing Coal. Nuclear magnetic resonance (NMR) is a new technology that can realize nondestructive analysis of the material's internal structure. It works on the principle of using the collection of hydrogen atoms that echo attenuation signals, using the SIRT inversion algorithm for mathematical inversion calculations to obtain the sample's spectrum, usually choosing the transverse relaxation time T_2 as a characterization signal.[26] This experiment used a MesoMR core magnetic imaging analyzer to realize the core analysis, and core imaging functions can also be used with a variety of self-developed hardware modules (liquid and gas injection modules, high-temperature and high-pressure circulation modules, osmosis adsorption modules, back-pressure modules, information acquisition modules, etc.) that can be realized under various conditions of the simulation study, and the test equipment is shown in Figure 2.

To investigate the microstructural changes of coal under different gas pressures, nondestructive testing of adsorbed gas coal samples was carried out using the NMR equipment. Due to the NMR gripper cavity and the coal body not reaching 100% fit, there is a particular gap between the two. To distinguish the free gas in the hole, the adsorption of gas in the coal body, and the free gas, it is necessary to perform the free

https://doi.org/10.1021/acsomega.3c08514
ACS Omega 2024, 9, 10468−10477

Figure 2. NMR analysis and the test system.

gas NMR spectral calibration experiments first. Gas adsorption experiments were carried out on Φ25 mm × 50 mm coal samples using NMR to obtain parameters such as the amount of gas adsorbed, the T_2 spectrum, and the pore size distribution of the coal samples. The specific experimental steps are as follows: (1) High-pressure helium was used to flush the chamber of the gripper in the NMR instrument and vacuum for 30 min to ensure that there is no leakage in the pipeline and then gradually adjust the gas pressure to 0, 0.7, 1.4, 2.1, and 2.8 MPa through the adjustment of the decompression valve and the pressure gauge, respectively, to collect and record the relevant experimental data. (2) Φ25 mm × 50 mm coal samples were put into the drying box, and the temperature of the drying box was set to 100 °C (the drying moisture of 100 °C used in this study would not change the physical structure of the coal body), and the time was set to 12 h. (3) After the chamber of the gripper was purged with helium, the dried coal samples were quickly put into the gripper, and the vacuum was applied to the gripper at 2.7 and 5 MPa peripheral pressures, respectively, after 30 min of evacuation. To minimize the variability of the coal samples, the adsorption experiments were carried out on the same piece of coal samples without removing the coal samples in the middle, and the gas adsorption experiments were carried out immediately after the gas pressure was set to 0.7, 1.4, 2.1, and 2.8 MPa in sequence. The relevant experimental data were recorded, respectively, after the adsorption equilibrium was reached.

2.3. Experimental Study on the Dynamic Mechanical Properties of Gas-Containing Coal. To simulate the storage environment of gas-containing coal seam with multiphysical field coupling, a dynamic mechanical test system for gas-containing coal was developed based on the SHPB equipment. The test system mainly comprises the SHPB main rod, hyperdynamic strain acquisition system, static load system, impact rod launching system, infrared velocimeter, perimeter pressure loading system, and gas charging and discharging system. Dynamic loading by the SHPB device launches the impact rod; the impact rod acts on the incident rod with a certain speed, and the stress wave propagates through the incident rod and acts on the specimen. The incident stress wave propagates in the incident rod; when the incident wave reaches the position of the specimen, part of the wave is reflected back to the incident rod, and part of the wave passes through the specimen to the transmission rod. Strain gauges affixed to the incident and transmission rods capture the incident, reflected, and transmitted waves. The static load system is realized mainly by fixing the incidence and transmission rods and clamping the specimen on a concentric axis between them. A gas charging and discharging system is included within the perimeter pressure loading system, and the unit's structure is shown in Figure 3. Compared with the SHPB

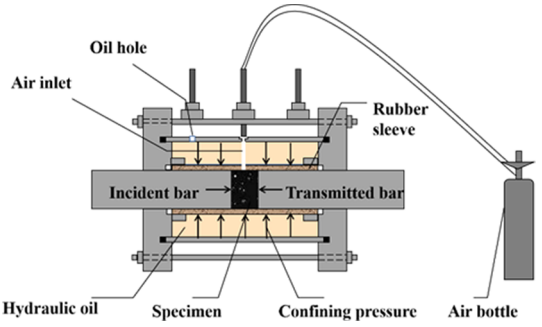

Figure 3. Triaxial confining pressure and gas pressure maintaining apparatus.

method of applying pressure around the gas, it is also possible to realize the function of gas filling and pressure retention. A rubber sleeve and an annular metal sleeve seal the specimen and part of the bar inside the metal cavity. Hydraulic oil is injected into the metal cavity to realize the confining pressure loading. At this time, the rubber sleeve tightly wraps the bars and specimen, forming a sealed space inside the sleeve, which can achieve the effect of pressure retention. Open the charging system, the gas from the cylinder through the pressure-reducing valve to the air intake, the specimen gradually absorbs the gas after entering the recess through the gas inlet and finally reaching the adsorption equilibrium, and the impact experiment can be carried out.

This paper tested the kinetic shock response of gas-containing coal under an axial static load, confining pressure, gas pressure, and shock load coupling to analyze the kinetic characteristics of gas-containing coal under combined dynamic and static loading. The loading conditions applied to the coal samples during the SHPB experiments are shown in Table 1.

3. RESULTS AND DISCUSSION

3.1. Results and Analysis of NMR Tests. *3.1.1. Principles of NMR Experiments.* Nuclear magnetic resonance experiments were performed by detecting the intensity of the nuclear magnetic signal obtained with the transverse relaxation time T_2 as a characterization signal whose relaxation time is proportional to the pore radius of the coal body, and its expression is as follows:

https://doi.org/10.1021/acsomega.3c08514
ACS Omega 2024, 9, 10468−10477

Table 1. Experimental Conditions and Results

serial number	axial static load/MPa	confining pressure/MPa	gas pressure/MPa	impact air pressure/MPa	dynamic strength/MPa			average dynamic strength/MPa
					1#	2#	3#	
1	2.7	5	0	0.9	167.30	169.10	167.50	167.97
2	2.7	5	0.7	0.9	154.80	150.10	153.80	152.90
3	2.7	5	1.4	0.9	147.70	148.43	143.20	146.44
4	2.7	5	2.1	0.9	139.71	138.50	133.40	137.20
5	2.7	5	2.8	0.9	123.90	120.30	122.81	122.34

$$\frac{1}{T_2} \approx \rho_2(S/V) = F_S\frac{\rho_2}{r} \quad (1)$$

$$r = cT_2 \quad (2)$$

where F_S is the pore-slit geometry factor of coal (F_S = 3 in spherical; F_S = 2 in columnar and plate), ρ_2 is the relaxation rate of the coal surface, which is a parameter characterizing the nature of the coal/rock, r is the pore radius, and c is the conversion factor.

From the above equation, it can be seen that the transverse relaxation time T_2 has a positive proportional relationship with the pore radius, and the size of the pore diameter can be distinguished by the difference in the transverse relaxation time T_2. In the gas adsorption T_2 curve, each T_2 time corresponds to a gas signal amplitude in the vertical coordinate axis, so the actual gas adsorption amount in the coal body can be expressed according to the integral value of the T_2 curve. The gas adsorption law and the pore structure change inside the coal body can be quantitatively investigated. The results of the NMR T_2 spectrum calibration experiments of free-state gas under different gas pressures are shown in Figure 4, and the T_2 spectrum curves of the gas within the coal samples under different gas pressures when the gas reaches the adsorption equilibrium are shown in Figure 5.

From Figure 4, it can be seen that the lateral relaxation time T_2 of the free-state gas and the integral area of the free-state gas T_2 spectrum increase when the gas pressure inside the gripper chamber gradually increases. In the gas pressure range of 0.7−2.8 MPa, the transverse relaxation time of free-state gas is concentrated in the range of 80−1180 ms. It can be seen that there is only one characteristic peak in the T_2 spectrum curve of free-state gas, which is consistent with the results of the study by Liu et al.[12] From Figures 4 and 5, it can be seen that the transverse relaxation time range of free-state gas in the free-state gas NMR calibration experiments is concentrated in the range of 180−1000 ms, and it can be determined that the P3 peak in Figure 5 is the free-state gas spectral peak. From eq 2, it can be seen that the micropore size corresponds to the smaller T_2 value, so the lateral relaxation time of adsorbed gas in the micropores is smaller than the lateral relaxation time of free gas in the macropores, and the other two peaks, P_1 and P_2, are the peaks of adsorbed and free gas spectra, respectively.

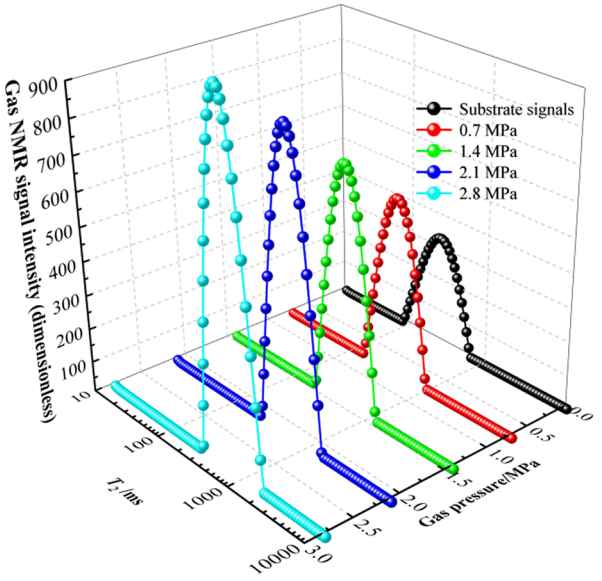

Figure 4. T_2 curves of free gas under different gas pressures.

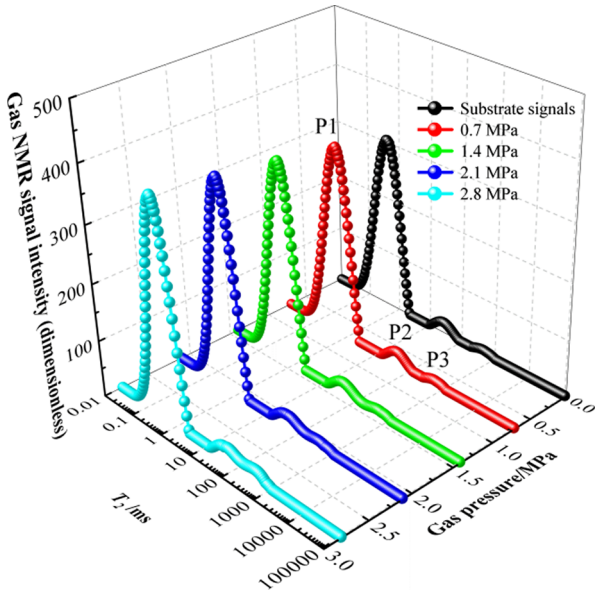

Figure 5. T_2 spectrum of coal gas adsorption balance under other gas pressures.

3.1.2. Effects of Adsorbed and Free Gas on the Pore Structure of Coal Samples under Different Gas Pressures. To further investigate the relationship between the gas pressure and the adsorbed and free- state gas, the adsorption peak area of T_2 mapping was calculated under different gas pressures, in which the effect of gas pressure on the adsorbed state gas is shown in Table 2, and the effect of gas pressure on free-state gas is shown in Table 3.

Table 2. Impact of Gas Pressure on Absorbed Gas

gas pressure/MPa	0.7	1.4	2.1	2.8
T_2 spectrum range/ms	0.3−2.5	0.3−2.5	0.3−2.5	0.3−2.5
adsorption peak area	378.15	396.54	423.31	442.65

https://doi.org/10.1021/acsomega.3c08514
ACS Omega 2024, 9, 10468−10477

Table 3. Impact of Gas Pressure on Free Gas

gas pressure/MPa	0.7	1.4	2.1	2.8
T_2 spectrum range/ms	10.6−130.3	10.8−141.5	10.5−160.38	11.4−212
free peak area	1065.34	1367.75	1955.01	2891.63

From Table 2, it can be seen that with the increase in gas pressure, the increase in gas adsorption is different. When the gas pressure was gradually increased from 0.7 to 1.4, 2.1, and 2.8 MPa, the increase in its gas pressure value was 100, 50, and 33.3%, respectively, and the corresponding increment of the adsorbed state gas was 18.39, 6.8, and 4.6%, respectively. In the early adsorption stage, as the gas pressure increases, the amount of adsorbed gas increases and the increment of adsorbed gas gradually decreases. The increase in adsorbed gas volume is large during the initial phase of gas pressure increase and decreases rapidly thereafter. It is analyzed that the distance between the molecules on the coal surface and the gas molecules decreases when the gas pressure increases from 0.7 to 1.4 MPa, but the mutual attraction between the molecules increases, which helps the coal to adsorb the gas. At this time, the adsorption amount increased more, reaching 18.39%. As the gas pressure rises, the distance between the gas molecules and coal surface molecules increases. The intermolecular force will be transformed into a repulsive force, which is not conducive to the adsorption of gas by the coal. The growth rate of gas adsorption decreases gradually.

From Table 3, it can be seen that when the gas pressure increases from 0.7 to 1.4, 2.1, and 2.8 MPa, respectively, the increase of the gas pressure value is 100, 50, and 33.3% in order, and the corresponding free gas increment is 28.39, 42.94, and 47.9% respectively. With the increase in gas pressure, both the amount of free gas and the gas increment increased. When the gas pressure increased from 0.7 to 1.4 MPa, the pore pressure of the macropores in the coal body was low, and with the increase of gas volume, the interior of the macropores was filled with free-state gas, and the increment of the free-state gas was 28.39%. As the gas pressure continues to rise, under the action of a higher gas pressure, the macropore orifices begin to expand, the gas density increases rapidly, and the gas increment becomes an upward trend.

The gas pressure increase has different degrees of influence on the micro- and macropores, and the lateral relaxation time of coal-adsorbed gas is positively proportional to the pore radius, as shown in eq 1. As the gas pressure increases, the lateral relaxation time of the microtubules is shorter, and the relaxation ranges from 0.3 to 2.5 ms in all cases. The lateral relaxation times of the macropores are not in the same time region, and the relaxation times appear to be "right-shifted", consistent with the findings of Tang et al.[27] This suggests that gas pressure does not have a significant effect on the microporous pore structure but has a significant dilation effect on the mesoporous pore structure.

3.2. Experimental Results of Dynamic Loading of Gas-Containing Coal under Different Gas Pressures.

3.2.1. SHPB Experimental Principle. When performing triaxial dynamic tests on gas-containing coal samples, the theoretical principles of the experiments still need to follow two basic premises: the one-dimensional stress wave theory and the assumption of stress homogenization.[28] During the dynamic loading process, the strain gauges on the incident and projected rods collect voltage signals and input them into the ultradynamic strain gauge. The strain−voltage conversion coefficients of the incident, reflected, and transmitted strains are brought into eq 3. The collected data are processed using the three-wave method to obtain the pressures and stresses of the coal samples,[28] respectively.

$$\begin{cases} \varepsilon(t) = \dfrac{C_0}{l_s}\displaystyle\int_0^t [\varepsilon_i(t) - \varepsilon_r(t) - \varepsilon_t(t)]\mathrm{d}t \\ \sigma(t) = \dfrac{AE}{2A_S}[\varepsilon_i(t) + \varepsilon_r(t) + \varepsilon_t(t)] \end{cases} \tag{3}$$

where $\varepsilon_i(t)$, $\varepsilon_r(t)$, and $\varepsilon_t(t)$ are the incident strain, reflected strain, and transmitted strain at moment t, dimensionless; l_s is the thickness of the specimen, m; C_0 and E are the longitudinal wave velocity and elastic modulus of the compression bar, m/s and MPa, respectively; A and A_S are the cross-sectional area of the compression bar and the cross-sectional area of the specimen, m^2, respectively.

3.2.2. Dynamic Mechanical Characterization of Gas-Containing Coal. According to the three-wave equilibrium equation theory, when the sum of incident stress and reflected stress equals the transmitted stress, the specimen satisfies the stress equilibrium condition in the loading process. The results of the stress waveforms at both ends of a typical specimen in the test are shown in Figure 6. It can be seen that the curve

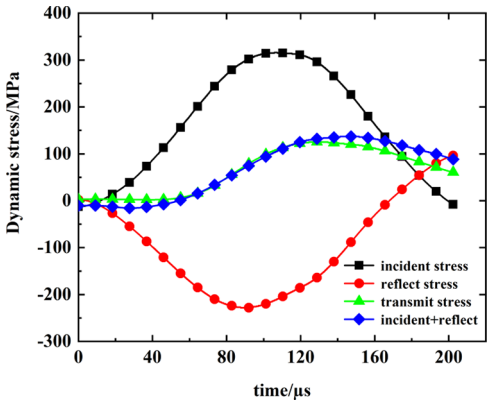

Figure 6. Dynamic stress balance.

formed by the incident wave and the reflected wave coincide with the stress curve of the transmitted wave, which indicates that the left and right ends of the specimen are subjected to equal stresses before destruction in the test process. The stress equilibrium conditions are satisfied,[29] which also indicates the validity of the test results. Figure 7 shows the dynamic stress−strain curve of gas-containing coal under different gas pressures.

From Figure 7, it can be seen that in the case of axial static load and confining pressure determination, with the increase of gas pressure, gas-containing coal samples in the dynamic compression process of the stress−strain curve with the change of gas pressure show noticeable differences and regularity. The test's axial static load and peripheral pressure parameters were small, and the smaller axial static load did not allow the cracks

https://doi.org/10.1021/acsomega.3c08514
ACS Omega 2024, 9, 10468−10477

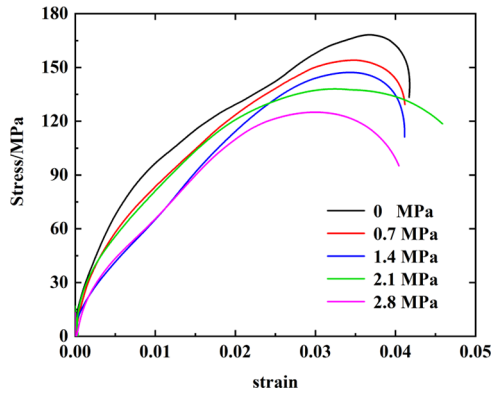

Figure 7. Dynamic stress−strain curve of gassy coal under different gas pressures.

inside the specimen to be completely compacted. However, higher loading rates cause the coal samples to leap over where the fissures are compacted and reach the elastic deformation stage directly during the dynamic loading process. With the increase in strain, the gas-containing coal samples showed irreversible deformation. The deformation of gas-containing coal mainly consisted of elastic and plastic deformations, and the plastic deformation accounted for the central part. The slope of the linear elastic phase of the stress−strain curve is maximum when the gas pressure is 0 under an axial static load and confining pressure. Since the slope of the linear elasticity stage at different gas pressures is affected by the discrete nature of the coal samples, the slope of the linear elasticity stage does not decrease linearly with the increasing gas pressure. Still, there is a decreasing trend, and the elastic modulus decreases. Wang et al.[30] also correlated the modulus of elasticity of coal samples under dynamic loading at different gas pressures, and the results showed that the modulus of elasticity of coal samples decreased with the increase of initial gas pressure. However, the correlation between gas pressure and elastic modulus was not well obtained in this paper, considering that the axial static load was applied along with the enclosing pressure, and the gas pressure did not affect the elastic modulus of the coal samples under suppression of the enclosing pressure.

The fitting curves between the dynamic strength and gas pressure of the coal samples in the five groups of experiments are shown in Figure 8. The dynamic compressive strength of gas-containing coal under impact loading shows a linear decrease with the increase of gas pressure, and the fitting degree can reach 0.96, respectively. The dynamic compressive strength was 169.1 MPa when the gas pressure was 0 and 123.9 MPa under 2.8 MPa gas pressure, which reduced the peak strength of the coal samples by 26.7% compared to the test results under no gas pressure. To further elaborate on the degree of deterioration of coal samples by gas, this paper defines a new damage parameter based on the dynamic compressive strength of gas-containing coals under a fixed axial load, confining pressure, and dynamic load to illustrate the degree of deterioration of the coal samples under the action of gas pressure:

$$D_S = \frac{\overline{\sigma_{S0}} - \sigma_{Si}}{\overline{\sigma_{S0}}} \times 100\% \quad (4)$$

where D_S is the rate of deterioration (%); σ_{S0} is the average dynamic strength of the coal sample when the gas pressure is 0, in units of (MPa); σ_{Si} is the dynamic strength of a specimen at any gas pressure in units of (MPa).

The degradation rate of the dynamic strength of the coal samples is shown in Table 4 when the gas pressure is 0. The degradation rate of gas pressure on the dynamic strength of the coal samples under a triaxial loading is zero. The average coal sample deterioration rate increased from 9 to 27% when the initial gas pressure was increased from 0.7 to 2.8 MPa. The average value of the deterioration rate of coal samples under different initial gas pressures was taken to fit the relationship between the initial gas pressure and the average deterioration rate, as shown in Figure 9. The average deterioration rate of coal samples increases linearly with the increase in gas pressure, which shows that the deterioration rate of coal

Table 4. Degradation of Peak Strength of Coal under Different Initial Gas Pressures

	D_S/%			
gas pressure/MPa	1#	2#	3#	$\overline{D_S}$/%
0	0.00	0.00	0.00	0.00
0.7	0.08	0.11	0.08	0.09
1.4	0.12	0.12	0.15	0.13
2.1	0.17	0.18	0.21	0.18
2.8	0.26	0.28	0.27	0.27

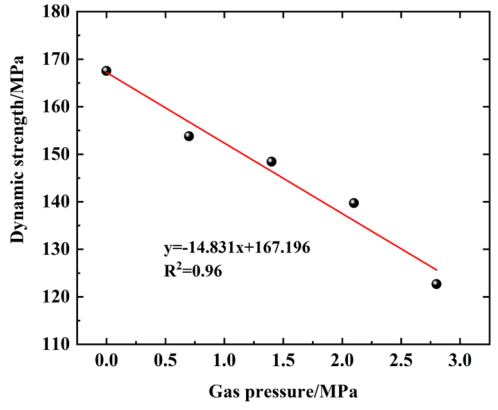

Figure 8. Change of dynamic mechanical indexes of gassy coal with gas pressure.

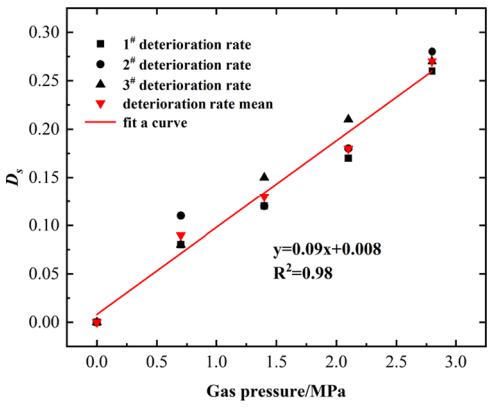

Figure 9. Relationship between the dynamic strength deterioration rate of coal samples and gas pressure.

https://doi.org/10.1021/acsomega.3c08514
ACS Omega 2024, 9, 10468−10477

samples increases with the increase in initial gas pressure. The main reason can be summarized as follows: the coal body under the joint action of adsorbed and free gas will undergo expansion and deformation and microcosmic damage such as micro-fissure sprouting and expansion, resulting in the reduction of the dynamic peak strength of gas-containing coal. The study of the mechanical properties of coal/rocks is of practical significance in understanding the hazards in mining operations, as it helps to predict and guard against potential geological hazards such as rock bursts, coal and gas outbursts, and roof collapses. By gaining a deeper understanding of the physical and mechanical properties of coal/rock, mining companies can develop more effective safety measures and engineering designs to minimize the risk of accidents, ensure the safety of workers and equipment, and increase the stability and efficiency of mining operations.

In this paper, the strain value corresponding to the peak intensity in the dynamic stress−strain curve of the specimen is taken as the failure strain, and its trend with the initial gas pressure is shown in Figure 10. The failure strain of gas-containing coals decreases linearly with increasing gas pressure with a goodness-of-fit of 0.94. The differences between the coal samples resulted in some dispersion in the failure strain of the coal samples at the same gas pressure. However, the failure strain tends to decrease with an increased gas pressure. This indicates that the increase in gas pressure weakened the dynamic compressive strength of the coal samples and that the samples were susceptible to damage at small deformations. The reason for this is mainly manifested in two aspects: On the one hand, the increase of gas pressure contains a certain kinetic energy of gas through the seepage effect into the pore fissures inside the coal samples, adsorbed in the coal matrix inside the coal samples. As the surface energy of coal samples adsorbed on gas decreases, the cohesion between coal matrices becomes weaker, and the spacing between particles becomes larger, reducing the ability of coal samples to resist deformation and damage. On the other hand, the free gas is transported between the pores and cracks inside the coal samples and acts as an expansion of the pore-crack structure.

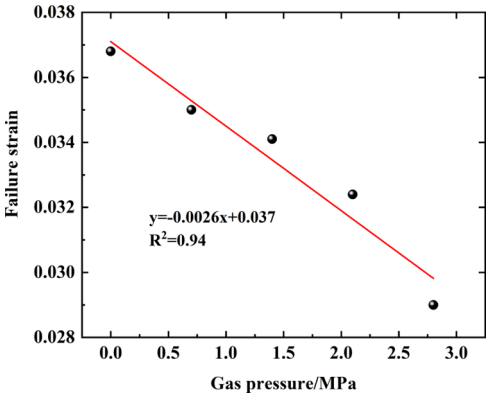

Figure 10. Relationship between failure strain and gas pressure in coal samples.

Under the joint action of adsorbed and free-state gas, the internal structure of coal samples undergoes expansion and deformation, microcrack expansion, and so forth, which weaken the mechanical properties of coal. In the impact experiments, the dynamic strength of the coal samples is reduced under the action of gas. Damage can be produced under small deformation, and the gas pressure has an important influence on the dynamic mechanical behavior of the coal samples. This shows that typical coal mine dynamic disasters such as rock bursts or coal and gas outburst in the gestation stage of the disaster, with the increase of pressure of the gas stored in the coal body, and the energy generated by a small dynamic load can cause deformation or even destruction of the coal body. In the underground coal mine, the weakening and erosion effect of gas on the coal body should be considered, and when the gas pressure of the coal seam is large, it is necessary to consider whether the critical value of the coal body for the occurrence of catastrophe becomes smaller and adjust the rock burst monitoring and warning indicators in time.

4. ANALYSIS OF THE EFFECT OF CHANGES IN THE PORE STRUCTURE OF GAS-CONTAINING COAL ON DYNAMIC MECHANICAL PROPERTIES

4.1. Stress State of Gas-Containing Coal Samples. The stress state of the gas-containing coal during the test is shown in Figure 11, where the specimen is first subjected to an axial static load and confining pressure. The gas then percolates inside the specimen at a constant pressure, and the presence of free-state gas in the cracks and pores of the specimen creates an outward pore gas pressure and expansion stresses due to the adsorbed state gas adsorbed in the coal matrix. Finally, the dynamic load is applied to the specimen, which induces destabilization damage to the specimen. On the one hand, the stress of dynamic load and three-dimensional stress acting together on the surface of the specimen is called total stress. On the other hand, because the gas pressure P acting in the pores of the specimen, i.e., the deformation damage of gas-containing coal, is determined by the average stress of external total stress, the pore gas pressure is called effective stress. The mathematical expression can be expressed as eq 5.

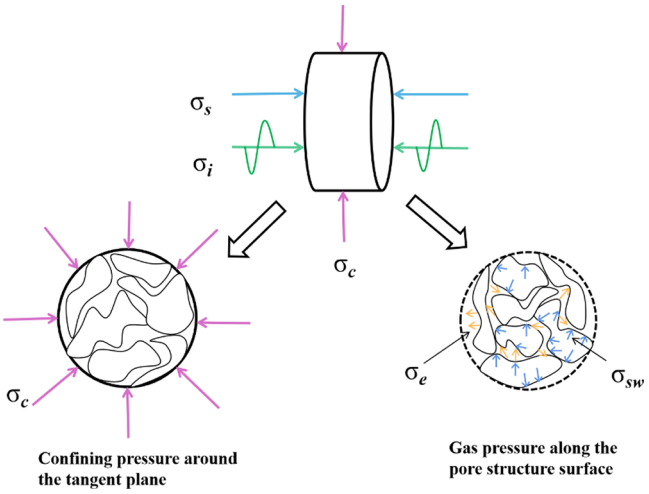

Figure 11. Stress state of gas-containing specimen (σ_s indicates axial static load; σ_c represents confining pressure; σ_i indicates dynamic load; σ_e is the expansion stress; σ_{sw} is the swelling stress).

$$\sigma_{(\text{eff})} = \sigma - \alpha p \tag{5}$$

where α is the pore gas pressure coefficient, also known as the Biot coefficient. However, in fact, the coal body also causes deformation of the coal matrix due to adsorbed gas, thus

https://doi.org/10.1021/acsomega.3c08514
ACS Omega 2024, 9, 10468−10477

causing adsorption swelling stresses. Li et al.[31] introduced adsorption swelling stresses σ_p in establishing the effective stress expression for gas-containing coal, with the following relationship:

$$\sigma_{(eff)} = \sigma - \alpha p - \sigma_p \quad (6)$$

It is known that coal under constraint conditions due to adsorption expansion will generate expansion stresses,[32] whose adsorption expressions are

$$\sigma_p = \frac{2a\rho RT(1-2\mu)\ln(1+bp)}{3V} \quad (7)$$

Changing the pore gas pressure P in eq 7 will give different adsorption swelling stress and adsorption expansion stress. As the initial gas pressure within the specimen increases, the gas pressure within the pore space increases and the amount of adsorbed gas in the coal matrix increases, leading to an increase in the adsorption expansion stress. From eq 7, it can be seen that when the pore gas pressure and adsorption swelling stress increase, the effective stress of the specimen decreases, and the strength decreases. When subjected to external forces, the force required to expand and destroy the fissures inside the specimen becomes smaller, and the specimen is more likely to break, and the greater is the risk of outbursts of coal and gas. This is consistent with the idea that there are complex connections and interactions between coal and gas obtained by Wu and Zhao.[32] Coal seams are the place where gas is stored, and the coal-forming process, period, and degree of metamorphism of coal seams also affect the composition and content of associated gas. Also, gas can have specific effects on the physical and mechanical properties of the coal body.

4.2. Influence of Changes in the Pore Structure of Gas-Containing Coal on Its Macroscopic Strength. When analyzing the variation of pore gas pressure with the strength of coal samples, it can be seen from Table 3 that when the gas pressure is increased from 0.7 to 1.4, 2.1, and 2.8 MPa, the lateral relaxation time of free gas ranges from 10.6 to 130.3, 10.8 to 141.5, 10.5 to 160.38, and 11.4 to 212 ms, respectively. The corresponding lateral relaxation times were calculated to be 119.7, 130.7, 149.88, and 200.6 ms. Assuming that the pore structure of coal samples is all-columnar pipes, the radius of macropores increases by 8.4, 14.7, and 33.8% in turn. Finally, the radius of macropores of coal samples increases by 0.63 times under 2.8 MPa gas pressure compared with 0.7 MPa gas pressure, corresponding to a decrease in the average dynamic strength from 152.9 to 122.3 MPa and a twofold increase in the deterioration rate of dynamic strength. The dynamic strength deterioration rate increased by 2 times. As the pore size of gas-containing coal increases, the effective stress acting on the coal sample by the confining pressure decreases, reducing the coal sample's ability to resist damage. To a certain extent, gas inhibits the compaction of pore cracks, favors their expansion, and weakens the friction coefficient between the macroscopic crack surfaces. The dynamic strength of coal samples decreased with the increase of pore gas pressure, and the deterioration rate of coal samples increased with the increase of pore gas pressure.

The effect of increasing the internal pore size of a coal body by gas pressure on its dynamic mechanical properties was further investigated. When the axial static load and confining pressure are specific, the relationship between the coal samples reaching dynamic compressive strength under impact loading and the loading time is shown in Figure 12. With the increase

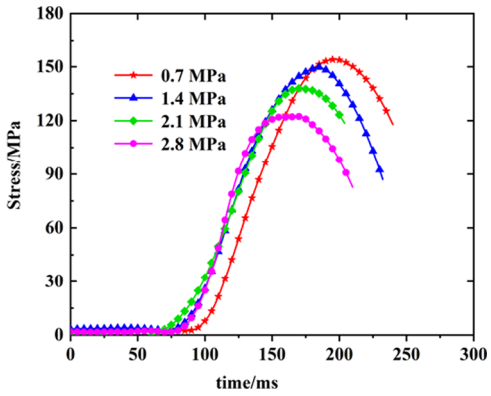

Figure 12. Relationship between failure strength and loading time.

of gas pressure to reach the destructive strength of the time required being less, this law and gas-containing coal fierce strength with the gas pressure change rule is consistent. The dynamic destruction time of gas-containing coal samples decreased with the increase of gas, and compared with the coal samples under the effect of 0.7 MPa gas pressure, the coal samples under the air pressure of 1.4, 2.1, and 2.8 MPa reached the decrease of the dynamic destruction time by 9.77, 17.20, and 33.31%, respectively. The coal samples chosen for the experiments had a weak propensity to impact but were still destroyed very sharply under the influence of gas pressure. This is because the influence of gas pressure on the large hole pore expansion effect is more obvious. The larger the gas pressure coal sample's internal pore cleavage radius is, the more the pore tip can withstand the plastic deformation. Subsequently, under the action of impact loading, the specimen under the influence of the stress wave will repeatedly experience the tensile and compressive force in a short period, which promotes the microfracture to continue to produce and expand, so the greater the gas pressure under the action of impact loading, the more prone is the destruction of the coal specimen, ultimately reaching destruction with a shorter time required. For the coal samples conforming to the rock dynamics experiments, the increase in gas pressure changed the coal samples' internal pore structure and degraded the coal body's mechanical properties, and the time to reach the dynamic damage was shorter. Based on this, for the real stress environment of coal seams, the present conclusions show that, for coal seams with a fixed depth of storage, the vertical in situ stress and horizontal principal stresses are unchanged. The gas pressure affects the time of the catastrophic process during the occurrence of the dynamic hazards and changes the intensity of the catastrophic events resulting from the dynamic hazards. The results of the study on the effect of gas pressure on the pore structure and dynamic mechanical properties of the coal body provide a theoretical basis for the assessment of rock bursts and gas disaster risk in deep mines and effective management. The mechanical properties of the coal body are deteriorated under higher gas pressure, and damage can occur with smaller loads. By mastering the mechanical laws in this case, it is possible to reduce the pressure on coal seams and rock seams by unloading as well as to reduce the risk of rock rupture. In addition, an in-depth understanding of these aspects can help develop more scientific mining strategies and improve the stability of the working environment, thereby reducing the risk of accidents and safeguarding the occupational health and safety of miners.

https://doi.org/10.1021/acsomega.3c08514
ACS Omega 2024, 9, 10468−10477

4.3. Future work. This work helps to improve the understanding of the law of the influence of gas pressure on the pore changes and dynamic mechanical properties of the coal body. It provides theoretical guidance for designing safe and efficient mining programs for coal resources under the mine. Strengthening gas monitoring technology and developing more advanced gas monitoring devices to monitor the concentration of dangerous gases in real time increase the sensitivity to potential dangers and thus take timely measures to avoid accidents. For gas pressure, there is a need to strengthen the monitoring of the gas content in the mine, and when the gas pressure is higher than the safe mining index of 0.74 MPa, gas pumping is the most effective and preferred method. For dynamic loads that lead to disasters, measures can be taken according to different dynamic loads. For example, when there is a mining area with a hard and thick roof, the roof prestitting technology can be used to reduce the accumulation of elastic energy, and when there is a geological tectonic area with fault slip, the mining speed should be slowed down and the geological exploration should be strengthened. Finally, a comprehensive risk assessment model is established to predict potential hazards and take appropriate safety measures, taking into account various factors, such as mine geology, processes, and equipment. Of course, this paper considers only the change of pore size and the change characteristics of dynamic mechanical indexes of coal samples under the change of gas pressure, which is of reference significance for mines with high gas concentrations. If the geological conditions of the coal seam change, then the results may differ. Future research should consider factors such as the stress environment and the magnitude of dynamic loads assigned to the coal seam and develop different technical equipment to conduct physical simulation tests based on these factors.

5. CONCLUSIONS

This paper investigated the effects of different gas pressures on the pore size structure and dynamic mechanical property change characteristics of coal samples using nuclear magnetic resonance (NMR) equipment and a self-developed gas-containing gas-dynamic−static coupled loading mechanical test system. The main research results are as follows:

(1) Gas pressure significantly affects the mass of adsorbed and free gas in the pore and fracture structure and the size of the pore and fracture in the coal samples. Still, the degree of influence on the micropore structure endowed with adsorbed gas and the macropore structure given with free gas is different. The effect of gas pressure on the tiny pore structure is insignificant, and there is a significant dilativity effect on the macropore structures.

(2) The dynamic strength and destructive strain of coal samples correlate with the magnitude of the gas pressure. Under the same triaxial stress, the deformation of gas-containing coal mainly consists of elastic deformation and plastic deformation. With the increase in the gas pressure, the dynamic compressive strength and destructive strain of the coal body decreased linearly. The degree of deterioration of the dynamic strength of the coal samples by gas was characterized by introducing a deterioration rate. The coal samples' deterioration rate showed a linear trend with the gas pressure increase. The gas pressure played a deteriorating role in the dynamic mechanical properties of the coal samples.

(3) At 2.8 MPa gas pressure compared to 0.7 MPa gas pressure, its macroporous pore radius increased by 0.63 times. The higher the gas pressure, the more pronounced the increase in the pore radius of the gas-containing coal samples is. Compared with the coal samples under 0.7 MPa gas pressure, the decrease in the arrival time to the destruction of the coal samples under 1.4, 2.1, and 2.8 MPa gas pressures was 9.77, 17.20, and 33.31%, respectively. The larger the gas pressure, the more limited the plastic deformation that the tips of the pores and cracks of the coal samples can withstand, and the more prone they are to destruction under the impact loading, the shorter the dynamic destruction time is.

AUTHOR INFORMATION

Corresponding Author

Sheng Xue − *School of Safety Science and Engineering and Joint National-Local Engineering Research Centre for Safe and Precise Coal Mining, Anhui University of Science and Technology, Huainan, Anhui 232001, China*; Email: sheng.xue@aust.edu.cn

Authors

Xin Gao − *School of Safety Science and Engineering and Joint National-Local Engineering Research Centre for Safe and Precise Coal Mining, Anhui University of Science and Technology, Huainan, Anhui 232001, China*; orcid.org/0009-0000-3857-6740

Weiyu Li − *School of Safety Science and Engineering, Anhui University of Science and Technology, Huainan, Anhui 232001, China*

Yidan Han − *School of Safety Science and Engineering, Anhui University of Science and Technology, Huainan, Anhui 232001, China*

Guangcheng Liu − *Shandong Succeed Mining Safety Engineering Co., Ltd., Taian, Shandong 271000, China*

Complete contact information is available at: https://pubs.acs.org/10.1021/acsomega.3c08514

Notes

The authors declare no competing financial interest.

ACKNOWLEDGMENTS

The authors are grateful to the Key Program of the National Natural Science Foundation of China (51934007) and the Open Research fund of the Joint National-Local Engineering Research Centre for Safe and Precise Coal Mining (EC2021018).

REFERENCES

(1) Yuan, L. Theory and technology considerations on high-quality development of coal main energy security in China. *Bull. Chin. Acad. Sci.* **2023**, *38*, 11−22.

(2) Yuan, L. Study on the development strategy of coal mine safety in China. *China Coal* **2021**, *06*, 1−6.

(3) Yuan, L. Research progress of mining response and disaster prevention and control in deep coal mines. *J. China Coal Soc.* **2021**, *46* (3), 716−725.

(4) Hu, S.; Wang, E.; Liu, X. Effective stress of gas-bearing coal and its dual pore damage constitutive model. *International Journal of Damage Mechanics* **2016**, *25* (4), 468−490.

(5) Wang, L.; Xue, Y.; Cao, Z.; et al. Experimental study on mode I fracture characteristics of granite after low temperature cooling with liquid nitrogen. *Water* **2023**, *15* (19), 3442.

(6) Xue, Y.; Ranjith, P. G.; Gao, F.; et al. Experimental investigations on effects of gas pressure on mechanical behaviors and failure

https://doi.org/10.1021/acsomega.3c08514
ACS Omega 2024, 9, 10468−10477

characteristic of coals. *Journal of Rock Mechanics and Geotechnical Engineering* **2023**, *15* (2), 412−428.
(7) Shoujian, P.; Jiang, X.; Dong, L. Experimental study on the influence factors of coal-containing gas during the fracture process. *Disaster Adv.* **2012**, *5* (4), 1385−1389.
(8) Zhang, Z.; Zhang, R.; Wu, S.; Deng, J.; Zhang, Z.; Xie, J. The stress sensitivity and porosity sensitivity of coal permeability at different depths: a case study in the Pingdingshan mining area. *Rock Mechanics and Rock Engineering* **2019**, *52*, 1539−1563.
(9) Kong, X.; Wang, E.; Li, S.; Lin, H.; Zhang, Z.; Ju, Y. Dynamic mechanical characteristics and fracture mechanism of gas-bearing coal based on SHPB experiments. *Theoretical and Applied Fracture Mechanics* **2020**, *105*, No. 102395.
(10) Yao, Y.; Liu, D.; Che, Y.; Tang, D.; Tang, S.; Huang, W. Petrophysical characterization of coals by low-field nuclear magnetic resonance (NMR). *Fuel* **2010**, *89* (7), 1371−1380.
(11) Jia, G.; Yang, M.; Zhang, X.; Liu, L. Experimental Study on the Pore Structure of Middle-and Low-Rank Coal and Its Influence on Methane Adsorption. *Geofluids* **2022**, *2022*, No. 1372243.
(12) Liu, J.; Jia, G.; Chen, S.; Ma, Q. Nuclear magnetic resonance experimental study on gas adsorption characteristics of deep low rank coal. *Coal Sci. Technol.* **2019**, *47* (9), 68−73.
(13) Yang, M.; Liu, L.; Liu, J.; Hong, L.; Mao, J.; Chai, P. LNMR experimental study on influence of confining pressure on gas adsorption laws of high rank coal. *J. Min. Saf. Eng.* **2020**, *37* (6), 1274−1281.
(14) Xu, Y.; Wu, X. Experimental Study on Influence of Gas Pressure on Adsorption Characteristics and Structure of Coal. *Saf. Coal Mines* **2019**, *50* (8), 1−4.
(15) Griffith, W. A.; Becker, J.; Cione, K.; Miller, T.; Pan, E. 3D topographic stress perturbations and implications for ground control in underground coal mines. *International Journal of Rock Mechanics and Mining Sciences* **2014**, *70*, 59−68.
(16) Ranathunga, A. S.; Perera, M. S. A.; Ranjith, P. G. Influence of CO2 adsorption on the strength and elastic modulus of low rank Australian coal under confining pressure. *International Journal of Coal Geology* **2016**, *167*, 148−156.
(17) Perera, M. S. A.; Ranathunga, A. S.; Ranjith, P. G. Effect of coal rank on various fluid saturations creating mechanical property alterations using Australian coals. *Energies* **2016**, *9* (6), 440.
(18) Gao, B.; Lv, P.; Guo, F. Study on mechanical properties and acoustic emission characteristics of coal at different gas pressure. *Coal Sci. Technol.* **2018**, *46* (01), 112−119.
(19) Wang, D.; Zhang, H.; Wei, J.; Wu, Y.; Zhang, H.; Yao, B.; Zhao, L. Dynamic evolution characteristics of gasbearing coal fractures under the influence of gas pressure based on industrial CT scanning. *J. China Coal Soc.* **2021**, *11*, 3550−3564.
(20) Liang, B.; Zhang, M.; Pan, Y.; Wang, Y.Experimental study of the effect of gas on the mechanical properties and mechanical response of coal. *Chin. J. Geotech. Eng.* **1995**, *05*.
(21) Yin, Z.; Chen, Z.; Chang, J.; Hu, Z.; Ma, H.; Feng, R. Crack initiation characteristics of gas-containing coal under gas pressures. *Geofluids* **2019**, *2019*, No. 5387907.
(22) Zhong, K.; Zhao, W.; Qin, C.; Gao, H.; Chen, W. Mechanical properties of roof rocks under superimposed static and dynamic loads with medium strain rates in coal mines. *Applied Sciences* **2021**, *11* (19), 8973.
(23) Yang, Z.; Liu, C.; Zhu, H.; Xie, F.; Dou, L.; Chen, J. Mechanism of rock burst caused by fracture of key strata during irregular working face mining and its prevention methods. *International Journal of Mining Science and Technology* **2019**, *29* (6), 889−897.
(24) Wang, E.; Feng, J.; Zhang, Q.; Kong, X.; Liu, X. Mechanism of rock burst under stress wave in mining space. *J. China Coal Soc.* **2020**, *45* (1), 100−110.
(25) Dou, L.-M.; He, J.; Cao, A.-Y.; Kong, S.; Cai, W. Rock burst prevention methods based on theory of dynamic and static combined load induced in coal mine. *J. China Coal Soc.* **2015**, *40* (7), 1469−1476.
(26) Zhou, S.; Liu, D.; Cai, Y.; Yao, Y. Fractal characterization of pore−fracture in low-rank coals using a low-field NMR relaxation method. *Fuel* **2016**, *181*, 218−226.
(27) Tang, J.; Tian, H.; Yu, L. Experimental study of influence of gas pressure on coal shale gas adsorption characteristics based on nuclear magnetic resonance spectrum. *Rock Soil Mech.* **2016**, *37* (S2), 203−208.
(28) Song, L.; Hu, S. Two wave method and three wave method in SHPB data processing. *Explos. Shock Waves* **2005**, *25* (4), 368−373.
(29) Cheng, C.; Xue, S.; Han, Y. Experimental study on the mechanical behavior of coal under triaxial dynamic compression. *Minerals* **2022**, *12* (10), 1206.
(30) Wang, L.; Chen, L.; Liu, H. Dynamic behaviors and deterioration characteristics of coal under different initial gas pressures. *Rock Soil Mech.* **2023**, *44* (01), 144−158.
(31) Li, X. C.; Guo, Y. Y.; Wu, S. Y.; Nie, B. S. Relation between effective stress and swelling stress of coal body. *J. Liaoning Tech. Univ.* **2007**, *26* (4), 535−537.
(32) Wu, S. Y.; Zhao, W. Analysis of effective stress in adsorbed methane-coal system. *Yanshilixue Yu Gongcheng Xuebao/Chin J. Rock Mech. Eng.* **2005**, *24* (10), 1674−1678.

https://doi.org/10.1021/acsomega.3c08514
ACS Omega 2024, 9, 10468−10477